Hindawi
Journal of Nanomaterials
Volume 2023, Article ID 6553200, 9 pages
https://doi.org/10.1155/2023/6553200

Research Article

Enhancing the Mechanical Properties of AZ31D Alloy by Reinforcing Nanosilicon Carbide/Graphite

Itha Veeranjaneyulu,[1,2] **Vemulapalli Chittaranjan Das**,[3] **and Srikanth Karumuri**[4]

[1]*Department of Mechanical Engineering, Acharya Nagarjuna University, Guntur, India*
[2]*Department of Mechanical Engineering, Aditya Engineering College, Surampalem, India*
[3]*Department of Mechanical Engineering, R.V.R. and J.C. College of Engineering, Guntur, India*
[4]*Department of Mechanical Engineering, Mizan Tepi University, Teppi, Ethiopia*

Correspondence should be addressed to Itha Veeranjaneyulu; anjimech@gmail.com and Srikanth Karumuri; srikanth.karumuri@mtu.edu.et

Received 7 September 2022; Revised 9 November 2022; Accepted 25 April 2023; Published 22 May 2023

Academic Editor: N. Senthilkumar

Magnesium-based alloys were more prevalent in automobile applications owing to their mechanical properties, low mass, and density. However, its poor mechanical properties are restricting its applications. Therefore, the present study focuses on improving the mechanical properties of AZ31D alloy by reinforcing silicon carbide (SiC) and graphite (Gr) nanoparticles with weight fractions of 2%, 4%, and 6% using stir-casting technique. The microstructure analysis was performed using a scanning electron microscope. The elemental analysis was confirmed using energy-dispersive spectroscopy, and X-ray diffraction was used to study various phases in the nanocomposites. Further, the mechanical properties, such as microhardness, ultimate tensile strength, yield strength, and compression strength of the nanocomposites, were significantly improved by 53%, 59%, 62%, and 82%, respectively, as compared with base alloy.

1. Introduction

Nowadays, substantial research outcomes concentrate on the advancement of product demand for designing materials with low specific gravities, lightweight materials, and with high strengths [1]. It was brought on by technical advancements, particularly in the aviation designing field. Magnesium alloys (specific gravity: 1.7 g/cm^3) appear to meet these standards. The exploration of magnesium (Mg) was a substitute for iron, polymers, and aluminum [2, 3]. Due to its low weight, Mg and its alloys have become popular materials for usage in products, including computer parts, recreational goods, aircraft components, home appliances, and vehicles, in recent years. Zinc and aluminum are alloyed with Mg material to enhance their mechanical properties and form group Mg–Al–Zn [4]. AZ31 is widely used in Mg–Al alloys. This structural material has a lot of potential for the aviation sector because of its less density and strong mechanical characteristics [5, 6]. However, the improvement in properties for AZ31 alloys is still challenging. Therefore, the nanocomposites play a vital role to enhance the mechanical, corrosion, and wear properties. Different methods were used to fabricate the nanocomposites [7–9]. Among different methods, stir casting is easy and economical compared to other methods to fabricate the metal matrix composites (MMC's) [10].

Several researchers have fabricated MMC's using stir-casting technique by mixing the various reinforcements. Khandelwal et al. [11] studied various weight proportions of $(Al_2O_3)_{np}$ on AZ31 and concluded that there was improvement in the tensile properties of nanocomposites. Torabi Parizi et al. [12] fabricated AZ80/calcium/aluminum oxide nanocomposite through stir-casting method. The results reveal that stir composite had more agglomerated particles than rheo composite and that stir composite had higher mechanical characteristics. Singh et al. [13] studied friction stir welding joint made of AZ61 alloy and reported that the microhardness of AZ61 is more in the thermo-mechanically impacted zone but lower in the stir zone. Rogal et al. [14] fabricated AZ91 nanocomposites by injection technology. The nanocomposites had hardness and compressive strength that were raised by 29% and 18%,

Figure 1: Stir-casting set up.

respectively. Subramani et al. [15] studied the microstructure of AZ31 alloy and the effect of SiC_{np} in composites. Further, the authors reported significant changes in mechanical properties with lamellar structure. The mechanical characteristics of metal matrix nanocomposite were investigated by Nourbakhsh et al. [16], and the findings revealed that the nanocomposites exhibited better qualities than base alloys. The effectiveness of composite materials reinforced with nanoscale and microscale graphene was studied by Vahedi et al. [17]. The results are shown that the particles are uniformly distributed and improved the mechanical properties. Huang et al. [18] investigated WS_2 reinforcement with different matrix materials and concluded that they reduced the secondary phases and enhanced the properties of 0.2 wt% WS_2. Huang et al. [19] studied Al_2O_3 and Sic nanoparticles in hybrid composites. The results have improved the ultimate tensile strength (UTS), yield strength (YS), and hardness. Silicon carbide particles were utilized as support in the magnesium network, which improves hardness, and strength in composites. By strengthening different particles, some researchers have been investigating unique techniques to enhance the properties of aluminum zinc series alloys [20, 21]. However, still enhancing the mechanical properties is challenging.

The novel feature of the work is the use of stir casting to reinforce SiC/Gr particles in AZ31D nanocomposites, improving their mechanical properties. As far as we are aware, stir casting has rarely been used in the manufacturing of nanocomposites. The mechanical properties of reinforced nanocomposites and evaluations of the microstructure were investigated using different techniques. All these results were compared with the AZ31D magnesium alloy. Overall, the present results are potential for the biomedicine and aviation industry.

2. Materials and Methods

2.1. Materials and Fabrication of Composites. In the experiment, AZ31D was employed as the matrix material, and silicon carbide and graphite particles with an average sizes of 75 and 53 nm, respectively, were used as reinforcements. Figure 1 illustrates the manufacturing of nanocomposites using the stir-casting technique. Figure 2 depicts the schematic view of the stir-casting setup. Table 1 provides the AZ31D alloy's chemical composition. AZ31D alloy makes into small pieces, poured in a muffle furnace, and set in a graphite crucible to overcome the chemical reactions while matrix material is in the liquid state. The raw materials and crucibles are heated to eliminate different gases and defects in castings. The crucible is preheated to 400°C in the muffle furnace and stacked with the material by increasing the

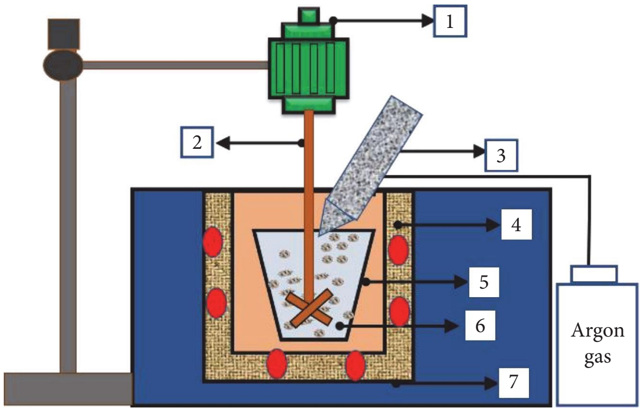

FIGURE 2: Schematic view of stir-casting method.

TABLE 1: Elements of AZ31D in wt%.

Elements	Al	Zn	Mn	Cu	Fe	Si	Mg
wt%	3	0.98	0.01	0.02	0.001	0.01	Rest

TABLE 2: Designation of specimens.

S. no.	Specimens	Compositions
1	S1	AZ31D
2	S2	AZ31D + 2% SiC + 2% graphite
3	S3	AZ31D + 4% SiC + 4% graphite
4	S4	AZ31D + 6% SiC + 6% graphite

temperature to 650°C. To prevent atmospheric oxidation, argon gas was used to create a vacuum environment in the furnace [22].

The flux 1 wt% of the matrix is used to prevent oxidation. The vortex made by a traditional stirrer worked at a speed of 700 rpm, and the stirring time is 15 min, which was run by an electronic variance. The prewarmed (200°C) reinforcements are included in the pool's center created by the moving process.

After increased sustenance, the liquid metal was filled in the preheated die. The specimens are quenched at room temperature for homogenization. Homogenization was carried out 24 hr to relieve stress. The designation of specimens is presented in Table 2.

2.2. Density and Porosity Measurement. The density of alloy and nanocomposites were evaluated using an experimental kit according to the ASTM: B962-13 standard [23] and it referred to Equation (1). The rule of the mixture method was applied to calculate the samples theoretical density using Equation (2). The percentage porosity of specimens was calculated using Equation (3) [24].

$$\text{Measured density (g/cc)} = \frac{\text{Weight of specimen in air}}{\text{Loss of weight in water}}, \quad (1)$$

$$\text{Theoretical density } (\rho_t) = \rho_m w_m + \rho_r w_r, \quad (2)$$

$$\text{Porosity (\%)} = \left(1 - \frac{\text{Measured density}}{\text{Theoretical density}}\right) \times 100, \quad (3)$$

where ρ_m = matrix density, ρ_r = reinforcement density, w_m = weight fractions of matrix, w_r = weight fractions of reinforcement.

2.3. Microstructure Characterization. The specimens were polished using different grades (500–2,000) of polishing paper by a disc polishing machine. Later, the samples were etched using a solution for 10–20 s. The microstructure of the base alloy and nanocomposites were investigated using a scanning electron microscope (SEM) (TESCAN and Model: VEGA3 SBH). Energy-dispersive spectroscopy (EDS) was used to know the existence of elements in the fabrication of the samples. X-ray diffraction (XRD) (Shimadzu, XRD-7000, and Japan) analysis was performed on the specimens to know the existence of different phases.

2.4. Mechanical Properties. Microhardness of the S1, S2, S3, and S4 were measured using Vickers's microhardness tester. During the testing, a load of 100 g for 10 s was applied to the specimen through a square-based diamond indenter, and the hardness readings were taken in a standard manner. The specimen was prepared (shown in Figure 3) as per the ASTM: E384 standard [25]. The experiment was repeated three times for each specimen and noted the average of three values.

Tensile and compressive properties are evaluated using UTM (INSTRON-E1025) with a strain rate of 3 mm/min. The specimen was prepared as per ASTM: E8 standard [26], and compression testing specimens were prepared as per ASTM: E9 standard [27], as shown in Figure 4. To get standardized values, the experiment was run three times for each specimen.

3. Results and Discussion

3.1. Microstructure Analysis. Figure 5 shows the microstructure analysis of AZ31D alloy and nanocomposites. Figure 4(a) represents α-Mg dendritic structure and the secondary phases surrounding grain boundaries [28]. Figure 5(b)–5(d) were shown the SEM images of nanocomposites with reinforcing of 2%, 4%, and 6% in weight fraction of SiC/Gr.

During the stirring process, it was noticed that SiC/Gr particles were evenly dispersed into the Mg matrix. There were no agglomerations occurred in the nanocomposites. Furthermore, the presence of reinforcements allowed for grain refining. A stronger mixing effect is produced by nanoparticles than by micron particles. Dendritic structures show a consistent distribution of particles with minimal porosity

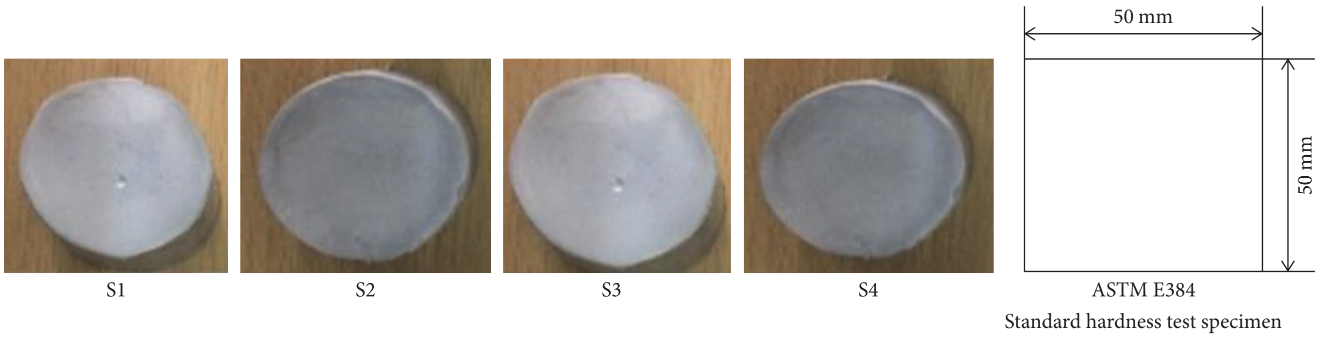

Figure 3: Specimens for microhardness test.

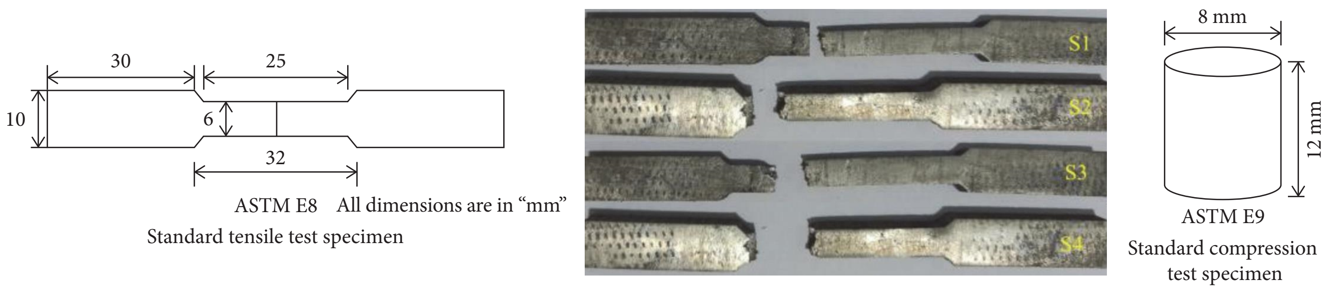

Figure 4: ASTM standards of tensile and compression test.

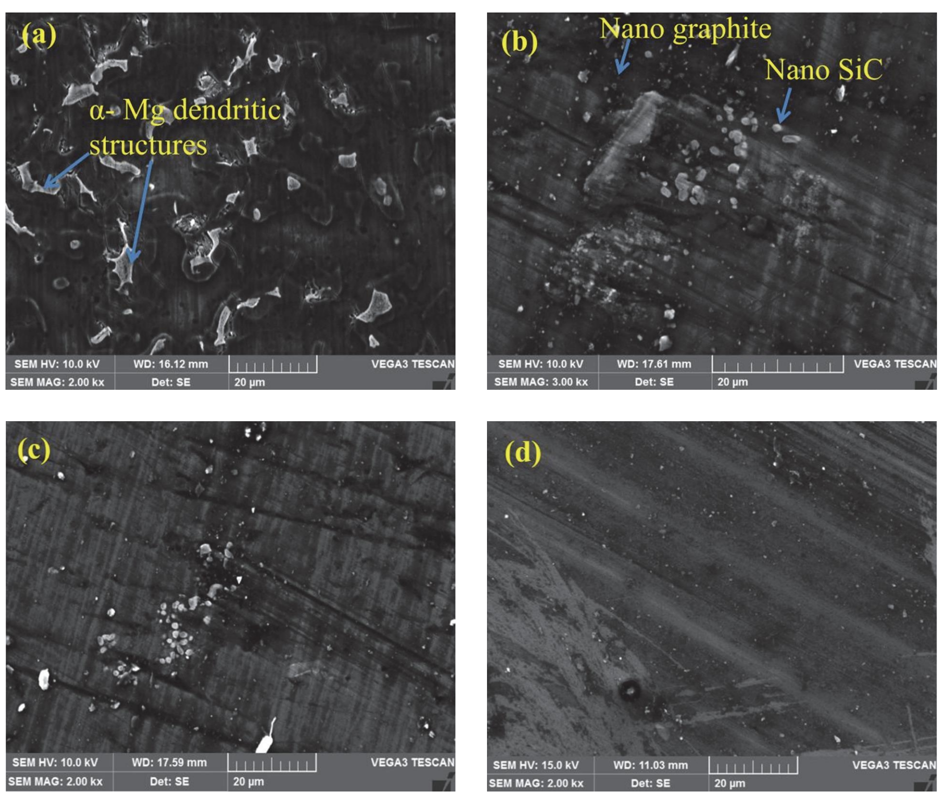

Figure 5: SEM images of (a) S1, (b) S2, (c) S3, and (d) S4 specimens.

and strong bonding between the AZ31D base alloy matrix and reinforcement. The reason for the little reduction in strength of the S4 nanocomposite was the porosity of the sample was increased compared to other nanocomposites.

EDS analysis revealed the presence of elements in AZ31D base alloy and nanocomposites, shown in Figure 6. Figure 6(a) shows the presence of aluminum (Al), zinc (Zn), and magnesium (Mg) elements in the AZ31D alloy.

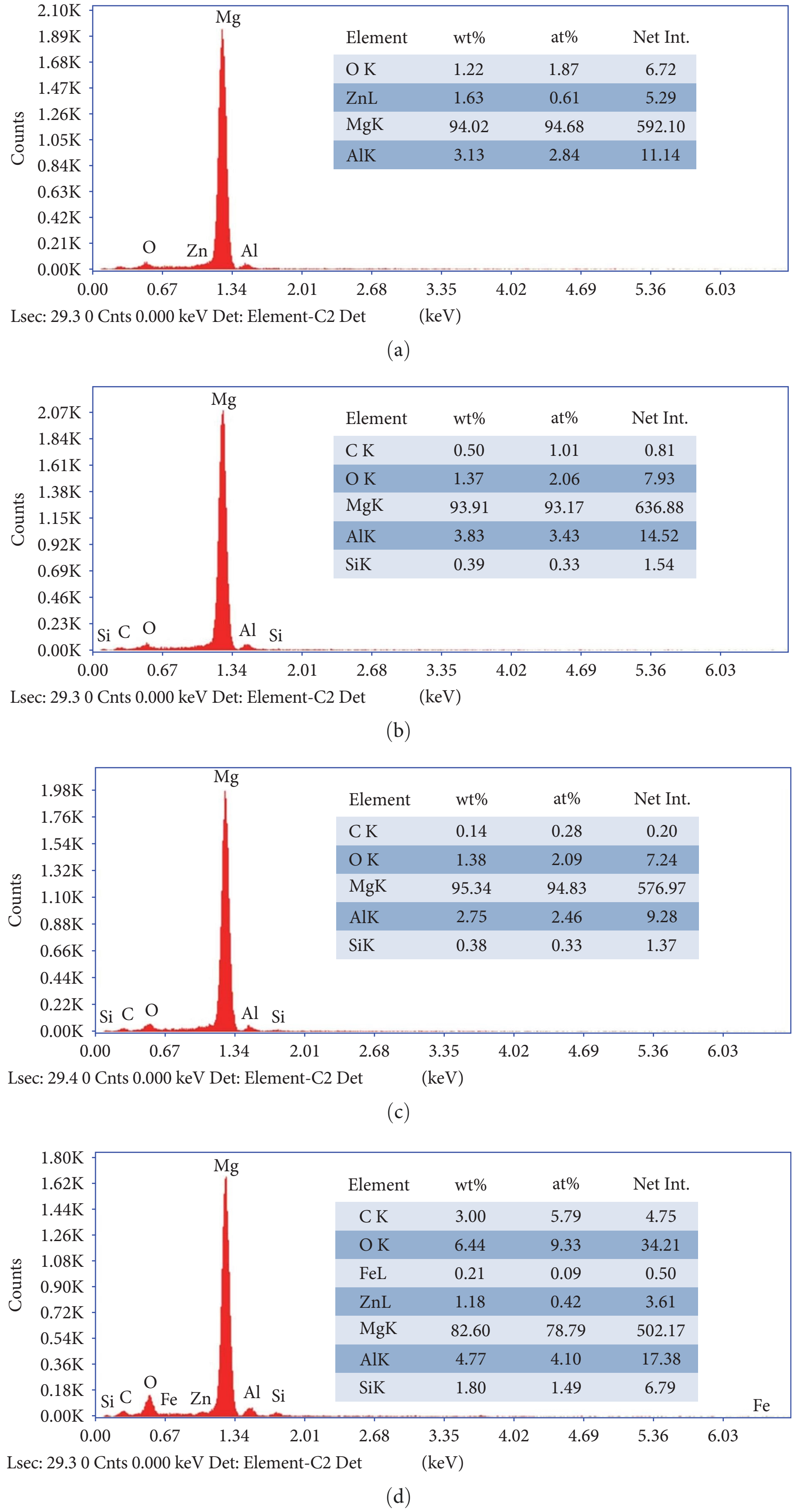

FIGURE 6: EDS analysis of (a) S1, (b) S2, (c) S3, and (d) S4 specimens.

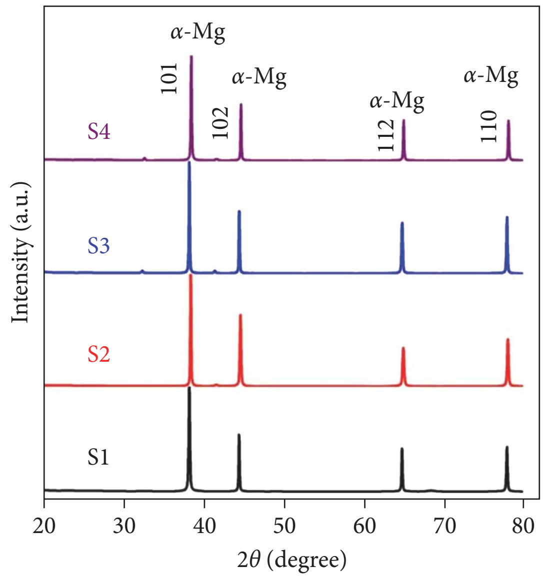

Figure 7: XRD spectrum of S1, S2, S3, and S4 specimens.

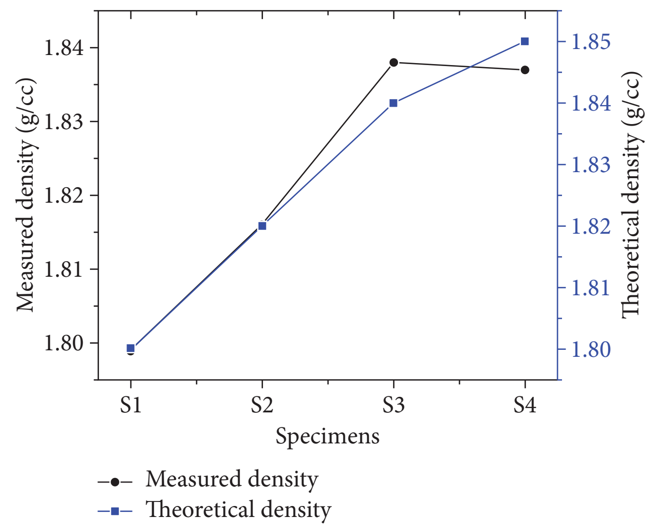

Figure 8: Variation of density for specimens.

Table 3: Density and porosity results.

Specimens	Theoretical density (g/cc)	Measured density (g/cc)	Porosity (%)
S1	1.8	1.799	0.05
S2	1.82	1.816	0.22
S3	1.84	1.838	0.11
S4	1.85	1.837	0.7

Table 4: Mechanical properties of AZ31D magnesium alloy and nanocomposites.

Specimens	Microhardness	UTS (MPa)	YS (MPa)	CS (MPa)
S1	71.89	102.3	65.09	173.42
S2	93.36	142.32	86.56	256.35
S3	98.89	162.94	105.25	315.56
S4	110	160.21	103.42	308.47

Figure 6(b)–6(d) shows the peaks of Al, Zn, Si, C, and Mg of the nanocomposite. The formation of magnesium oxide during the solidification process resulted in the peak of oxygen [29]. The impingement of the argon gas during the casting process prevents oxidation.

The XRD spectrums of the four specimens are illustrated in Figure 7. This analysis was used to identify the different phases and it indicates that α-Mg is the primary element that exists in the nanocomposite. The primary diffraction peaks (2θ) identified for α-Mg are 38.05°, 44.81°, 65.12°, and 78.23° [30], and the planes assigned for α-Mg peaks were (101), (102), (112), and (110). The peak intensity varies with varying weight fractions of SiC/Gr. Peak intensity increases with an increase in SiC/Gr wt% in AZ31D alloy. The base material is mainly composed of Mg in matrix form; the large peaks correspond to the parent AZ31D alloy.

3.2. Density and Porosity. The densities of the four specimens are illustrated in Table 3. The density of nanocomposites increased with decreased porosity as the increase particulates [24]. Here, the measured density was lower values as compared with the theoretical density due to the dispersion of atoms in the nanocomposite, as is represented in Figure 8. The S3 specimen exhibited less porosity than other nanocomposites. Therefore, it helps to improve the mechanical properties.

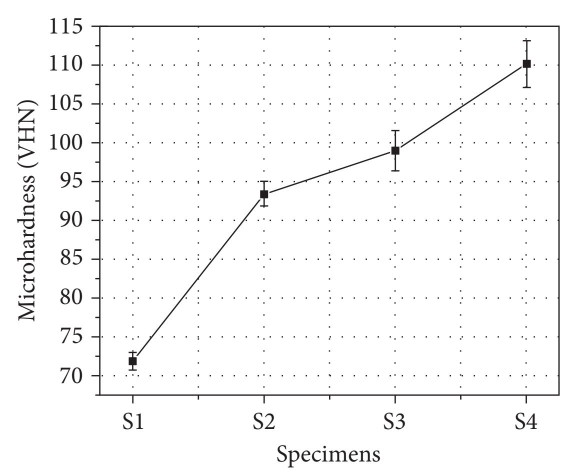

Figure 9: Microhardness of specimens.

3.3. Mechanical Properties. The mechanical properties of AZ31D alloy and nanocomposites are shown in Table 4. The microhardness of AZ31D alloy and nanocomposites are shown in Figure 9. The microhardness of the nanocomposite of the S4 specimen consists of a higher hardness value (110 VHN) as compared to AZ31D magnesium alloy (71.89 VHN). It shows clearly that the microhardness of nanocomposites exhibits 53% higher than the base alloy. The increase in hardness is

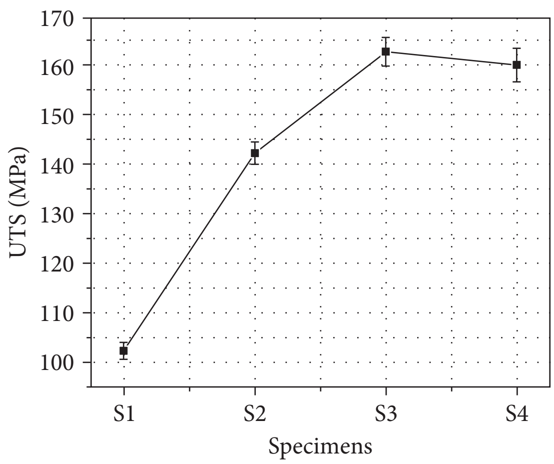

Figure 10: Ultimate tensile strength (UTS) of specimens.

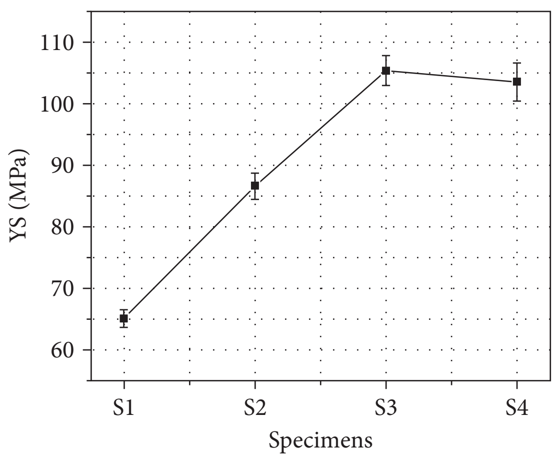

Figure 11: Yield strength (YS) of specimens.

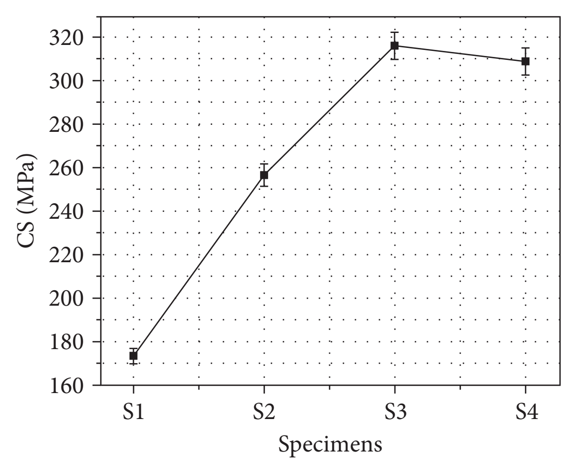

Figure 12: Compressive strength (CS) of specimens.

attributed due to the addition of reinforcement particles in the matrix. The grain refinements of nanocomposites were improved due to the uniform distribution of the reinforcement particles, and it was confirmed by the SEM images. During solidification, the functioning of grain boundary anchors and nucleation locations for new grains will occur [22]. The result of an increase in microhardness was limiting the mobility of the dislocations [31].

UTS, YS, and compression strength (CS) of nanocomposites are shown in Table 4. The tight interfacial connection between the matrix and reinforcement is crucial for improving the tensile properties. Figures 10–12 show a little reduction in the strength of the S4 nanocomposite compared to the S3 nanocomposite. It was due to the formation of fewer voids and cracks in the microstructural image of the S4 nanocomposite. Another reason was the reinforcements overstrained the lattice. The grain size of the reinforcements bonding between the reinforcements and matrix may affect the composite's strength [24, 29]. The increased weight fractions of reinforcement will lead to enhance in the mechanical properties of S2 and S3 nanocomposites. Overall, the UTS and YS were enhanced by 59% and 62%, respectively, as compared with the base alloy.

The nanocomposite's compressive strength varies depending on the particle size and how well the reinforcement bonds to the matrix [28, 32]. The superior strength is attained due to microstructural modifications. The reinforcement and matrix have a sufficient surface-to-surface bond, and the applied stress changes the matrix's interactions with the reinforced particles. The compressive strength of the alloy is 173.42 MPa, whereas improved compressive property was observed for the S3 nanocomposite because of the surface–surface bonding between reinforcement and matrix. Finally, by addition of SiC/Gr particles make more compressive strength, whereas the flexibility may reduce. Overall, the CS of nanocomposite was enhanced by 82% as compared with base alloy.

4. Conclusion

The results of the present investigation can be summarized as follows:

(i) AZ31D magnesium alloy and AZ31D-SiC-Gr nanocomposites with (2, 4, and 6 wt%) have been successfully fabricated using the stir-casting technique.

(ii) The microstructure analysis of AZ31D magnesium alloy and nanocomposites was performed. SEM images revealed the distribution of reinforcements in the matrix material, dendritic structure, grain boundaries, and defects in nanocomposites.

(iii) EDS analysis examined all the elements (Al, Zn, C, Si, and Mg) and their wt% and at% of the nanocomposites. XRD analysis provided complete information about phases of constitutes in the nanocomposites and indicated α-Mg was the primary element in the nanocomposite.

(iv) Microhardness of the nanocomposites was enhanced due to the presence of reinforcements. Finally, it was concluded that the nanocomposites were stabilized, and the load transformed equally to the entire nanocomposite.

(v) The porosity of the S3 specimen was exhibited less as compared with other nanocomposites. Therefore, the S3 specimen has shown better mechanical properties than other specimens.

(vi) UTS, YS, and CS were significantly enhanced by 59%, 62%, and 82%, respectively, due to the presence of SiC/Gr particles in the matrix. Perfect interfacial bonding and little clustering of reinforcement particles were attributed to improvement in tensile properties.

Based on the microstructure analysis and experimental investigations, concluded that the S3 nanocomposite has exhibited less porosity and better mechanical properties as compared to all other nanocomposites. The result of the present study was promising for the biomedicine and aviation industry.

Data Availability

The data used to support the findings of this study are available from the corresponding author upon request.

Conflicts of Interest

The authors declare that they have no conflicts of interest.

References

[1] P. Samal, P. R. Vundavilli, A. Meher, and M. M. Mahapatra, "Recent progress in aluminum metal matrix composites: a review on processing, mechanical and wear properties," *Journal of Manufacturing Processes*, vol. 59, pp. 131–152, 2020.

[2] M. Gupta and W. L. E. Wong, "Magnesium-based nanocomposites: lightweight materials of the future," *Materials Characterization*, vol. 105, pp. 30–46, 2015.

[3] R. Vara Prasad Kaviti, D. Jeyasimman, G. Parande, M. Gupta, R. Narayanasamy, and P. G. Koppad, "Improving the friction and wear characteristics of AZ31 alloy with the addition of Al_2O_3 nanoparticles," *Materials Research Express*, vol. 6, no. 12, Article ID 126505, 2019.

[4] S. You, Y. Huang, K. U. Kainer, and N. Hort, "Recent research and developments on wrought magnesium alloys," *Journal of Magnesium and Alloys*, vol. 5, no. 3, pp. 239–253, 2017.

[5] A. Dziubińska, A. Gontarz, K. Horzelska, and P. Pieśko, "The microstructure and mechanical properties of AZ31 magnesium alloy aircraft brackets produced by a new forging technology," *Procedia Manufacturing*, vol. 2, pp. 337–341, 2015.

[6] E. Suneesh and M. Sivapragash, "Comprehensive studies on processing and characterization of hybrid magnesium composites," *Materials and Manufacturing Process*, vol. 33, no. 12, pp. 1324–1345, 2018.

[7] S. K. Sharma and K. K. Saxena, "Effects on microstructure and mechanical properties of AZ31 reinforced with CNT by powder metallurgy: an overview," *Materials Today: Proceedings*, vol. 56, Part 4, pp. 2038–2042, 2022.

[8] A. K. Singh, S. Soni, and R. S. Rana, "A critical review on synthesis of aluminum metallic composites through stir casting: challenges and opportunities," *Advanced Engineering Materials*, vol. 22, no. 10, Article ID 2000322, 2020.

[9] I. Dinaharan, S. Zhang, G. Chen, and Q. Shi, "Development of titanium particulate reinforced AZ31 magnesium matrix composites via friction stir processing," *Journal of Alloys and Compounds*, vol. 820, Article ID 153071, 2020.

[10] A. Kumar, R. S. Rana, and R. Purohit, "Microstructure evolution, mechanical properties, and fractography of AA7068/Si_3N_4 nanocomposite fabricated thorough ultrasonic-assisted stir casting advanced with bottom pouring technique," *Materials Research Express*, vol. 9, no. 1, Article ID 015009, 2022.

[11] A. Khandelwal, K. Mani, N. Srivastava, R. Gupta, and G. P. Chaudhari, "Mechanical behavior of AZ31/Al_2O_3 magnesium alloy nanocomposites prepared using ultrasound assisted stir casting," *Composites: Part B: Engineering*, vol. 123, pp. 64–73, 2017.

[12] M. Torabi Parizi, A. Habibolahzadeh, and G. R. Ebrahimi, "Optimizing and investigating influence of manufacturing techniques on the microstructure and mechanical properties of AZ80-0.5Ca-1.5Al_2O_3 nanocomposite," *Materials Chemistry and Physics*, vol. 199, pp. 485–496, 2017.

[13] K. Singh, G. Singh, and H. Singh, "Investigation of microstructure and mechanical properties of friction stir welded AZ61 magnesium alloy joint," *Journal of Magnesium and Alloys*, vol. 6, no. 3, pp. 292–298, 2018.

[14] L. Rogal, B. Baran, P. Bobrowski, A. Tarasek, P. Ozga, and L. Litynska-Dobrzyńska, "Effect of nano-SiC on microstructure and mechanical properties of AZ91 magnesium alloy processed by thixomolding," *Solid State Phenomena*, vol. 285, pp. 133–138, 2019.

[15] M. Subramani, S.-J. Huang, and K. Borodianskiy, "Effect of SiC nanoparticles on AZ31 magnesium alloy," *Materials*, vol. 15, no. 3, Article ID 1004, 2022.

[16] S. H. Nourbakhsh, M. A. Shahrokhian, M. Hasanzadeh, and A. Atrian, "Investigation of mechanical and microstructural properties of AZ31/SiC nanocomposite fabricated by squeeze stir casting," *Materials Research Express*, vol. 5, no. 8, Article ID 086514, 2018.

[17] F. Vahedi, A. Zarei-Hanzaki, A. Salandari-Rabori, H. R. Abedi, A. Razaghian, and P. Minarik, "Microstructural evolution and mechanical properties of thermomechanically processed AZ31 magnesium alloy reinforced by micro-graphite and nano-graphene particles," *Journal of Alloys and Compounds*, vol. 815, Article ID 152231, 2020.

[18] S.-J. Huang, C.-C. Lin, J.-Y. Huang, and R. Tenne, "Mechanical behavior enhancement of AZ31/WS_2 and AZ61/WS_2 magnesium metal matrix nanocomposites," *Advances in Mechanical Engineering*, vol. 10, no. 2, pp. 1–14, 2018.

[19] S.-J. Huang, M. Subramani, and C.-C. Chiang, "Effect of hybrid reinforcement on microstructure and mechanical properties of AZ61 magnesium alloy processed by stir casting method," *Composites Communications*, vol. 25, Article ID 100772, 2021.

[20] M. Subramani, S.-J. Huang, and K. Borodianskiy, "Effect of WS_2 nanotubes on the mechanical and wear behaviors of AZ31 stir casted magnesium metal matrix composites," *Journal of Composites Science*, vol. 6, no. 7, Article ID 182, 2022.

[21] N. Anand and S. Senthil Kumaran, "Development and influence of tribomechanical properties on magnesium based hybrid metal matrix composites—a review," *Materials Research Express*, vol. 7, Article ID 036520, 2020.

[22] J. Pradeep Kumar, D. S. Robinson Smart, S. Manova, and N. Ummal Salmaan, "Effect of TaC/Ti/Si_3N_4 hard ceramics on mechanical and microstructural behaviour of AA7075 processed through stir casting process," *Advances in Materials Science and Engineering*, vol. 2022, Article ID 6804011, 13 pages, 2022.

[23] ASTM Standard B962-13, *Standard Test Methods for Density of Compacted or Sintered Powder Metallurgy (PM) Products*

Using Archimedes' Principle, ASTM International, West Conshohocken, PA, USA, 2013.
[24] A. H. Khan, S. A. A. Shah, F. Umar et al., "Investigating the microstructural and mechanical properties of novel ternary reinforced AA7075 hybrid metal matrix composite," *Materials*, vol. 15, no. 15, Article ID 5303, 2022.
[25] ASTM Standard E384, *Standard Test Method for Knoop and Vickers Hardness of Materials*, ASTM International, West Conshohocken, PA, USA, 2013.
[26] ASTM Standard E8, *Standard Test Methods for Tension Testing of Metallic Materials*, ASTM International, West Conshohocken, PA, USA, 2013.
[27] ASTM Standard E9, *Standard Test Methods for Compression Testing of Metallic Materials*, ASTM International, West Conshohocken, PA, USA, 2013.
[28] B. Saleh, J. Jiang, R. Fathi, Q. Xu, L. Wang, and A. Ma, "Study of the microstructure and mechanical characteristics of AZ91–SiCp composites fabricated by stir casting," *Archives of Civil and Mechanical Engineering*, vol. 20, Article ID 71, 2020.
[29] S. Sharma, J. Singh, M. K. Gupta et al., "Investigation on mechanical, tribological and microstructural properties of Al–Mg–Si–T6/SiC/muscovite-hybrid metal–matrix composites for high strength applications," *Journal of Materials Research and Technology*, vol. 12, pp. 1564–1581, 2021.
[30] U. Rokkala, S. Bontha, M. R. Ramesh, V. K. Balla, A. Srinivasan, and S. V. Kailas, "Tailoring surface characteristics of bioabsorbable Mg–Zn–Dy alloy using friction stir processing for improved wettability and degradation behavior," *Journal of Materials Research and Technology*, vol. 12, pp. 1530–1542, 2021.
[31] V. K. Soni and A. K. Sinha, "Effect of alloying elements, phases and heat treatments on properties of high-entropy alloys: a review," *Transactions of the Indian Institute of Metals*, vol. 76, pp. 897–914, 2023.
[32] K. C. K. Kumar, B. R. Kumar, and N. M. Rao, "Microstructural, mechanical characterization, and fractography of AZ31/SiC reinforced composites by stir casting method," *Silicon*, vol. 14, pp. 5017–5027, 2022.